www.sensorsportal.com

Sensors & Transducers
Published by IFSA Publishing, S. L., 2021
http://www.sensorsportal.com

A Model for Electrical Properties Measurement of Graphene-based Composites with an Open-ended Coaxial Probe Technique

[1, *] **Hind BAKLI,** [2] **Mohamed MOUALHI and** [3] **Mourad MAKHLOUF**
[1] Laboratory of Electronics and Electrical Systems Engineering,
BP 48 Cherchell, Tipaza, 42006, Algeria
[2] Laboratory of Software Implementation and Validation, Algiers, 16000, Algeria
[3] Laboratory of Combustion, Detonation and Ballistic, BP 48 Cherchell, Tipaza, 42006, Algeria
[1] Tel.: + 213671614893
E-mail: baklih@yahoo.com

Received: 29 October 2021 /Accepted: 28 November 2021 /Published: 30 November 2021

Abstract: Electrical properties measurement of graphene-based composite materials in the frequency range 1-18 GHz is proposed in this paper. These materials have been prepared by adding different mass percentages ranging from 1 to 40 % of graphene to PVC. The measurement setup is based on the association of an open-ended coaxial probe and a vector network analyzer. A modeling based on a modified calibration one port model and capacitive approach is proposed to relate the measured microwave signal to the complex permittivity and conductivity of the material under test.

Keywords: Dielectric permittivity, Microwave characterization, Open-ended coaxial probe, Graphene, Polymer.

1. Introduction

Excellent properties of graphene-based polymer composites [1-2] including high flexibility, good thermal and electrical conductivity, low temperature processing conditions, and simple fabrication process have allowed its use in different applications such as electronic devices, electromagnetic shielding, photovoltaic cells, sensors, supercapacitors, Li ion batteries, protective coating, biomedical applications and water purification, etc. [3-5].

The knowledge of electrical properties of conductive polymer materials is required when using these materials, especially at high frequencies. These properties have been measured using different microwave techniques including resonant cavities, open-ended coaxial probe, waveguides and transmission lines based methods. Since it has the advantages of being non-destructive to the materials, the ability of wideband measurement and the easiness of sample preparation, the open-ended coaxial probe technique is the most commonly used one. This technique consists of placing an open-ended coaxial transmission line in contact with a sample so that the electrical fields around the end of the probe interact with the sample under test and measuring changes in the reflection coefficient affected by the electromagnetic properties of the sample [6-7].

In this paper, a calibration model based on a modified conventional one port calibration and lumped elements models is proposed to retrieve the graphene-based composite materials electrical properties from measured reflection coefficient measured when using an open-ended coaxial probe.

The modified one port calibration model is used to relate the measured reflection coefficient to the one at the aperture-plane of the probe. Capacitive approach is used to model the open-ended aperture admittance when a composite material is set to the probe contact and thus to relate the reflection coefficient at the aperture-plane to the electrical properties of the material. The permittivity and conductivity of the prepared graphene-based composite materials are experimentally extracted using the proposed model in the frequency range 1-10 GHz.

2. Modeling of the Probe-sample Interaction

When the open-ended probe is placed in the vicinity of the sample, its electromagnetic properties affect the detection system parameters. A modeling of the structure under investigation which represents the interaction between the probe and the sample is then used to retrieve the electromagnetic properties of the sample from the parameters measured by the detection system.

In this work, a homemade open-ended probe (the inner diameter of the outer conductor is D= 4.1 mm and the diameter of the inner conductor is d= 1.3 mm) is used to characterize different graphene-based composite materials. We present in Fig. 1 the simulated distribution at a frequency of 2.45 GHz of the electrical field at the end of the coaxial probe. From this figure, we notice that the field is concentrated around the open end of the probe. Thus, lumped elements model can be used to describe the interaction between the open-ended probe and the material under test. Thus, the aperture admittance can be modeled as two parallel capacitors, as illustrated in Fig. 2.

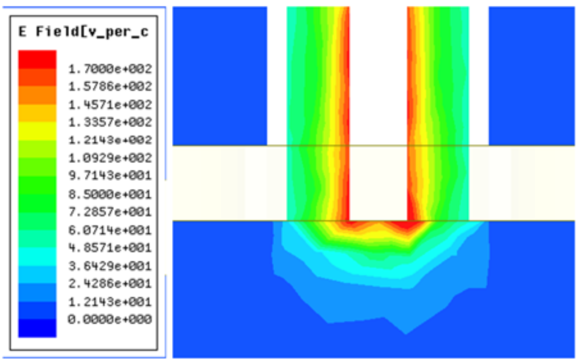

Fig. 1. HFSS™ simulation of the electric field magnitude - F = 2.45 GHz.

From this model, the open-ended aperture admittance Y_{MUT} can be obtained by the following equation

$$Y_{MUT} = j\omega\left(C_f + \varepsilon_r C_0\right), \tag{1}$$

where C_f is the capacitance determined by fringing-fields effects inside the probe, C_0 is the capacitance that is related to the microwave coupling between the probe and the composite material, ω is the angular frequency and ε_r is the complex permittivity of the material.

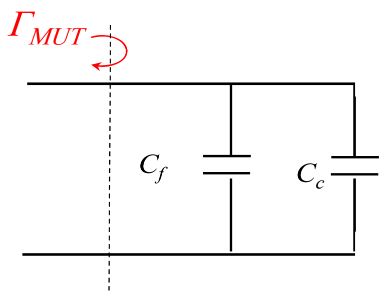

Fig. 2. Lumped elements model for open-ended coaxial probe.

3. Experimental Procedure

3.1. Sample Preparation

In this work, we used graphite (as electrodes) and electrolyte baths (electrochemical cell) composed of sulfuric acid and water for the exfoliation process. Thus, we performed the electrochemical exfoliation of graphite in sulfuric acid to obtain high quality and large-area graphene thin sheets.

In a typical electrochemical process, a two-electrode system has been used in which a graphite rod acts as an anode and another rod acts as a cathode in a solution of sulfuric acid H_2SO_4. The electrolyte consisted of 100 ml of aqueous solution with a volume ratio of 1/4 of H_2SO_4 and H_2O. A DC voltage of 10 V was applied until the total consumption of the graphite rod which was converted to graphene sheets within 1.5 hours.

The aqueous solution of graphene ink was centrifuged and washed several times with distilled water after sonication for half an hour. Finally, our graphene is dried for 24 hours at 333 °K. After drying our graphene electrochemically (GE) this material is subjected to a microwave treatment for 30 seconds to separate the sheets of graphene from each other, the latter will be named (GE-MW).

Polyvinyl chloride (PVC SIGMA ALDRICH, 98 %) was used as a polymer matrix. A mass of graphene ranging from 0 % to 40 % was dispersed for 15 minutes in an emulsion of dibutyl sebaceate (DBS) under ultrasonic vibration. A mass of PVC was added to the mixture (G/DBS) and finally, the mixture was subjected to a heat treatment at 423 °K for 1 h 30. In order to study the effect of loads on the properties of PVC, a series of nanocomposites were made and the elaborate compositions are summarized in Table 1.

The experimental part of this research includes the preparation of the raw material, graphene (G) with electrochemical method.

Table 1. Compositions and mass fractions of engineered nanocomposites.

PVC	DBS	G
45 %	55 %	0 %
45 %	54 %	1 %
45 %	53 %	2 %
45 %	51 %	4 %
45 %	49 %	6 %
45 %	47 %	8%
45 %	45 %	10 %
45 %	35 %	20 %
45 %	25 %	30 %
45 %	15 %	40 %

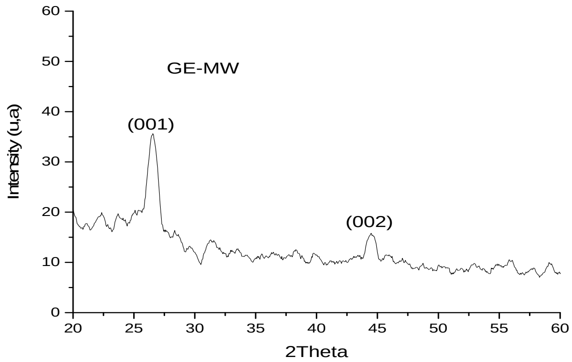

Fig. 4. XRD patterns of GE and GE-MW.

Our samples were analyzed with X-ray diffraction. This technique allows the analysis of the crystalline phases contained in a sample. Information on its microstructure (size of the crystallites, micro stresses) can also be extracted.

X-ray diffraction is based on the recording of a diffractogram, which allows you to identify / quantify the phases, calculate the crystallographic parameters and determine the average size of the crystallites by different methods (Scherrer, Williamson-Hall).

Our samples were analyzed using a D8 Advance Eco diffractogram (Bruker) operating with a copper tube (λ = 1.54Å)

The X-ray spectrum of the graphite powder (Fig. 3) shows the hexagonal structure according to the (002) orientation, as revealed by the single peak at 2θ = 25° which corresponds to a spacing of about 3, 4 A° between the graphite planes.

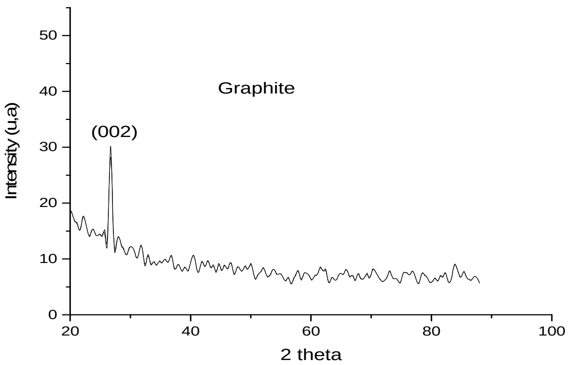

Fig. 3. XRD patterns of Graphite XRD.

The graphene X-ray spectra (GE-MW) (Fig. 4) show the absence of the diffraction peak in comparison with graphite (2θ = 26.4°). This indicates the removal of the periodicity in the structure of Graphene exfoliated. In fact, the increase in the inter-spacing following the oxidation of the graphite comes from the intercalation of the oxygen-containing groups between the layers of the graphite, thus weakening the van der Waals forces between the layers, which allow an exfoliation easy via sonification in an aqueous medium.

We present in Fig. 5 the scanning electron microscopy image of the graphene used in composites samples. This image shows the dynamic form of graphene and confirms the existence of homogeneity in the microscopic structure.

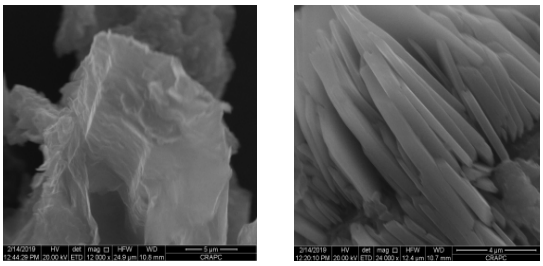

Fig. 5. SEM image of graphene.

3.2. Experimental Set-up

We present in Fig. 6, the experimental set-up based on the association of the homemade open-ended coaxial probe and a vector network analyzer (Rhode & Schwarz ZVL6). The power has been fixed to 0 dBm and then SOL calibration has been performed.

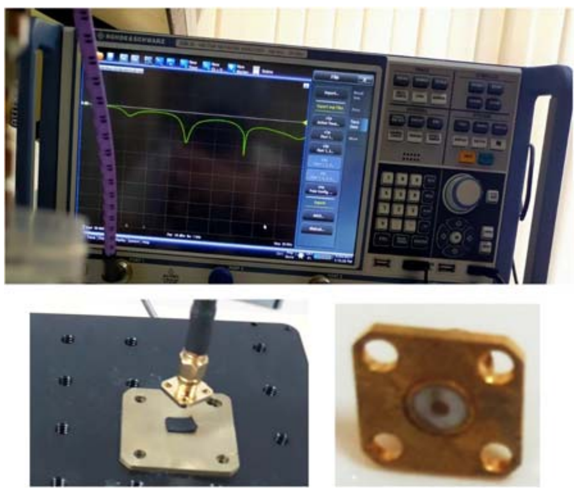

Fig. 6. Experimental set-up.

4. Calibration Model

To relate the measured reflection coefficient *Γ* to the desired reflection coefficient referenced at the end of the coaxial probe Γ_{MUT}, a phenomenological flow graph using a modified one-port calibration model (Fig. 7) is shown below.

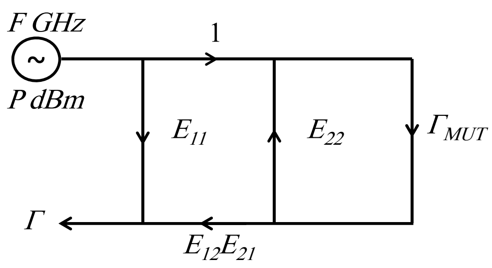

Fig. 7. Signal flow graph for a one port calibration model.

From this graph, the measured reflection coefficient *Γ* can be obtained by the following equation

$$\Gamma = E_{11} + \frac{E_{12}E_{21}\Gamma_{MUT}}{1 - E_{22}\Gamma_{MUT}}, \qquad (2)$$

where the complex terms E11, E12 E21 and E22 are calibration coefficients that correspond respectively to the directivity, source match and reflection tracking errors. The reflection coefficient Γ_{MUT} at the end of the probe is given by

$$\Gamma_{MUT} = \frac{Y_{MUT}(\varepsilon_r) - Y_0}{Y_{MUT}(\varepsilon_r) + Y_0}, Y_0 = \frac{1}{Z_0}, Z_0 = 50\Omega, \qquad (3)$$

where Y_{MUT} is the open-ended aperture admittance.

By combining the relations (1) to (3), we can get the following equation

$$\Gamma = \frac{A_2 + A_3\varepsilon_r}{A_1 - \varepsilon_r}, \qquad (4)$$

where A_1, A_2 and A_3 are three frequency-dependent complex constants, related to E_{11}, E_{12} E_{21}, E_{22}, Z_0, C_f and C_0.

Three materials (air, PTFE and de-ionized water) selected for calibration with known permittivity are used to solve the system (4) and determine A_1, A_2 and A_3. The material permittivity is then retrieved by inverting equation (4) for the different composites. The sample permittivity is given by $\varepsilon_r = \varepsilon' - j\varepsilon''$, where ε' and ε'' are the real and imaginary parts of dielectric permittivity. The conductivity of the composite material is then calculated using

$$\sigma = 2\pi f \varepsilon_0 \varepsilon'', \qquad (5)$$

where f is the frequency of measurement.

5. Results and Discussions

We present in Fig. 8, the different magnitude spectra of the reflection coefficient for the different composite materials prepared by adding to PVC different concentrations of graphene ranging from 1 to 40 %.

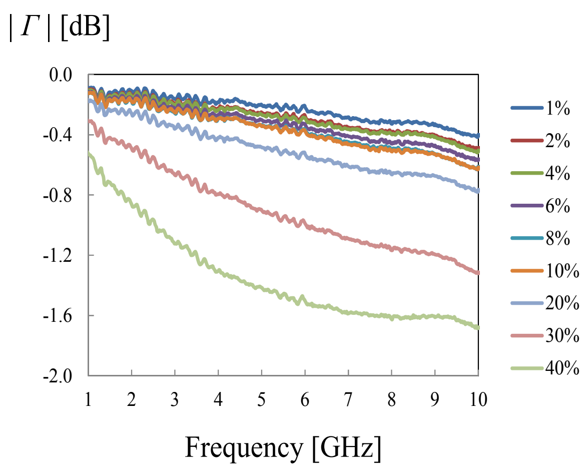

Fig. 8. Measured magnitude spectra of the reflection coefficient for different G-PVC composite materials.

It is clearly shown in Fig.8 that the different G-PVC composite materials are well differentiated by means of reflection coefficient magnitude. When the graphene concentration increases, the reflection coefficient magnitude decreases. This can be attributed to the electron motion hysteresis under an alternating electromagnetic field which induces additional polarization relaxation processes that increase the microwave absorption.

We present in Fig. 9 the experimentally determined dielectric permittivity for the different graphene-based composites. It is retrieved that as the concentration of graphene increases, the particles interaction within the polymer matrix increases. This results in higher polarization, and hence, a higher dielectric constant.

We present in Fig. 10 the measured real and imaginary parts of the permittivity and the conductivity at a test frequency of 2.45 GHz for the different samples.

From these graphs, it can be seen that for the different graphene-based composites, when the graphene concentration increases, the real and imaginary parts of permittivity and the conductivity increase. In fact, by increasing the graphene concentration, the interaction of the particles within the matrix goes up. The average polarization correlated to a cluster of particles is more robust than an individual particle due to the improved inclusion dimensions of the composite and thus a larger interfacial area, resulting in a higher average polarization, and thus a larger contribution to the dielectric properties and conductivity.

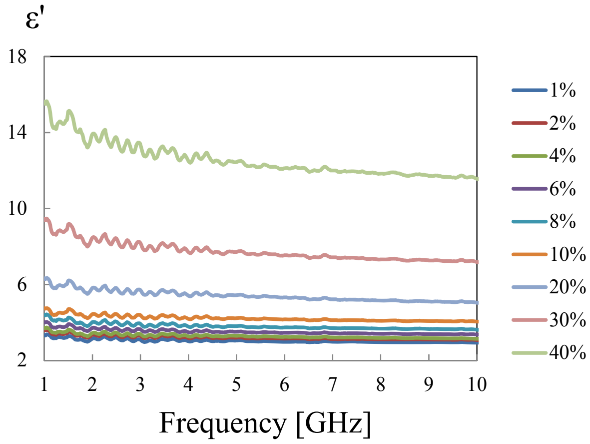

(a)

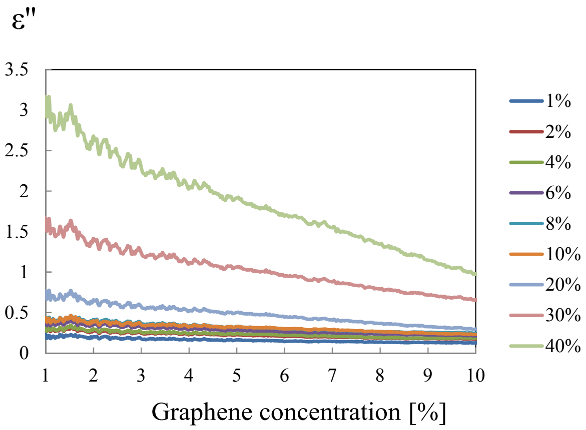

(b)

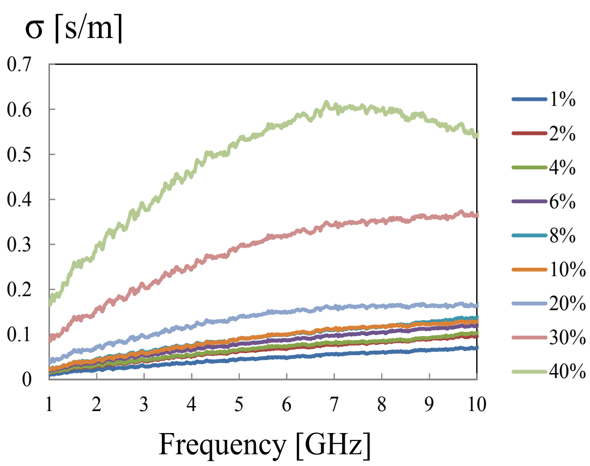

(c)

Fig. 9. Measured electrical properties of G-PVC composite materials. (a, b) real and imaginary parts of permittivity, (c) conductivity.

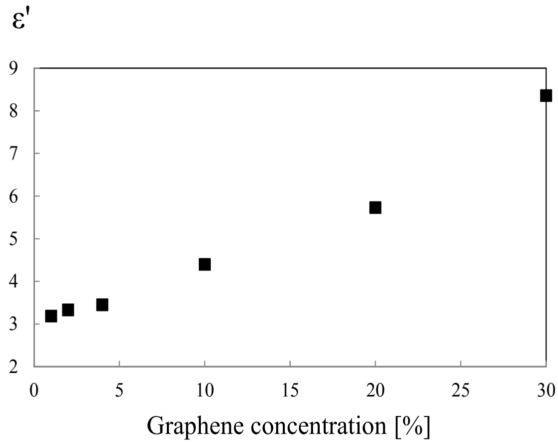

(a)

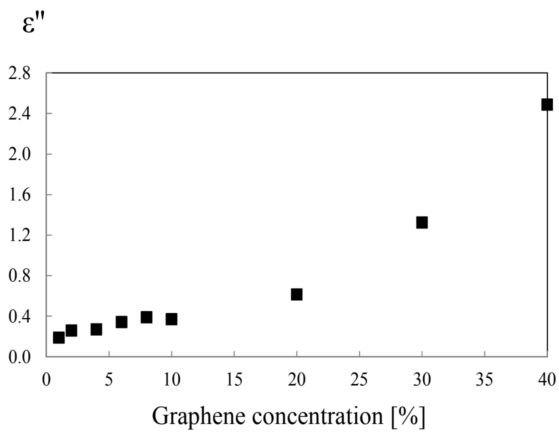

(b)

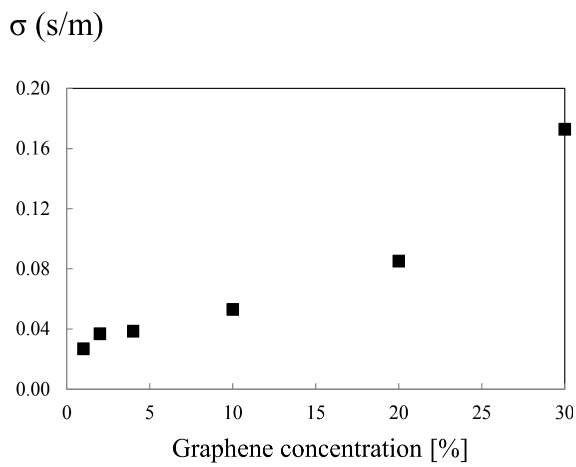

(c)

Fig. 10. Measured electrical properties of G-PVC composite materials. (a, b) real and imaginary parts of dielectric permittivity, (c) conductivity.

6. Conclusions

Electrical properties of Graphene-based composites have been experimentally determined using open-ended coaxial probe in the frequency band ranging from 1-10 GHz. A lumped elements model has been used to describe the interaction between the open-ended probe and the material under test. A modified one-port model has been proposed to relate the measured reflection coefficient to the electrical properties of the material. The results obtained show the capacity of the proposed method for wide-band characterization of composite materials.

Acknowledgements

Measurements have been done in the Signals and Systems Laboratory of the Institute of Electrical and Electronic Engineering, University M'hamed BOUGARA of Boumerdes, Algeria.

References

[1]. T. K. Das, S. Prusty, Graphene-Based Polymer Composites and Their Applications, *Polymer-Plastics Technology and Engineering*, Vol. 52, Issue 4, 2013, pp. 319-331.

[2]. X. Huang, C. Zhi, Y. Lin, H. Bao, G. Wu, P. Jiang, Y.-W. Mai, Thermal Conductivity of Graphene-based Polymer Nanocomposites, *Materials Science and Engineering: R: Reports*, Vol. 142, 2020, pp. 100577.

[3]. G. Wu, P. Tan, D. Wang, Z. Li, L. Peng, Y. Hu, C. Wang, W. Zhu, S. Chen, W. Chen, High-performance Supercapacitors based on Electrochemical-induced Vertical-aligned Carbon Nanotubes and Polyaniline Nanocomposite Electrodes, *Scientific Reports*, Vol. 7, Issue 1, 2017, pp. 1-8.

[4]. M. He, J. Jung, F. Qiu, Z. Lin, Graphene-based Transparent Flexible Electrodes for Polymer Solar Cells, *Journal of Materials Chemistry*, Vol. 22, Issue 46, 2012, pp. 24254.

[5]. W. Guo, J. Su, Y.-H. Li, L.-J. Wan, Y.-G. Guo, Nitroxide Radical Polymer/graphene Nanocomposite as an Improved Cathode Material for Rechargeable Lithium Batteries, *Electrochimica Acta*, Vol. 72, 2012, pp. 81-86.

[6]. H. Bakli, K. Haddadi, T. Lasri, Quantitative Determination of Small Dielectric and Loss Tangent Contrasts in Liquids, in *Proceedings of the on IEEE International Instrumentation and Measurement Technology Conference (I2MTC)*, Turin, Italy, 2017.

[7]. H. Bakli, M. Moualhi, M. Makhlouf, Electrical Properties Measurement of Graphene-based Composites using an Open-ended Coaxial Probe Technique, in *Proceedings of the 7th International Conference on Sensors and Electronic Instrumentation Advances (SEIA' 2021)*, Palma de Mallorca, Spain, 2021, pp. 72-75.